

X-520-70-398

NASA TM X- 65426

# A PROGRESS REPORT ON SCINTILLATION OBSERVATIONS AT ANCÓN AND JICAMARCA OBSERVATORIES

JOSÉ POMALAZA  
RONALD F. WOODMAN  
GILBERTO TISNADO  
JAIME SANDOVAL  
ALBERTO GUILLÉN

OCTOBER 1970



**GODDARD SPACE FLIGHT CENTER**  
**GREENBELT, MARYLAND**

**X71-10212**  
(ACCESSION NUMBER)

FF No. 602 (D)

29  
(PAGES)

TMX 65426  
(NASA CR OR TMX OR AD NUMBER)

(THRU)

F1  
(CODE)

29  
(CATEGORY)

AVAILABLE TO U.S. GOVERNMENT AGENCIES  
AND CONTRACTORS ONLY

A PROGRESS REPORT ON SCINTILLATION OBSERVATIONS  
AT ANCON AND JICAMARCA OBSERVATORIES

by

José Pomalaza  
Ronald F. Woodman  
Gilberto Tisnado  
Jaime Sandoval  
Alberto Guillén

October 1970

Goddard Space Flight Center  
Greenbelt, Maryland

## CONTENTS

|  | <u>Page</u> |
|--|-------------|
| ABSTRACT .....                                     | v           |
| INTRODUCTION .....                                 | 1           |
| DIVERSITY COMBINING TECHNIQUES .....               | 14          |
| ANALYSIS OF DATA .....                             | 16          |
| RECOMMENDATIONS FOR A SPACE DIVERSITY SYSTEM ..... | 24          |
| FUTURE WORK .....                                  | 25          |
| REFERENCES .....                                   | 25          |

PRECEDING PAGE BLANK NOT FILMED

A PROGRESS REPORT ON SCINTILLATION OBSERVATIONS  
AT ANCON AND JICAMARCA OBSERVATORIES

by

Jose' Pomalaza  
Ronald F. Woodman  
Gilberto Tisnado  
Jaime Sandoval  
Alberto Guillén

ABSTRACT

The distribution of scale sizes of the diffraction pattern produced by ionospheric irregularities responsible for satellite scintillations has been obtained. They have been derived from measurements of the time autocorrelation function of the fluctuations of the signals received from synchronous satellites and from drift velocities obtained by cross correlation methods using two spaced antennas. The sizes have been found to be of the order of 200 and not larger than 400 meters.

The scale sizes of the irregularities as well as the relative amplitude of the fluctuations, for the case of lower satellites, has been deduced from the measurements made with synchronous satellites using a full wave theory. It is found that, as the satellite gets closer to the layer of the irregularities, the scale size of the diffraction pattern on the ground gets larger. When the distance between the satellite and the layer becomes smaller than a Fresnel distance, the r.m.s. of the amplitude scintillations is largely reduced. The preferred heights of the layer of irregularities has been determined from radar measurements at Jicamarca.

It is recommended that the minimum distance between antennas for a space diversity reception system should be 300 meters for coverage of high altitude satellites and 1000 meters for coverage of all satellites. The maximum distance is limited by economical considerations and possible problems of real state. There is also a technical problem associated with very large spacing and the phase (or time delay) of the information received at both antennas, when the bandwidth of the modulation is large. This can be solved by a scheme which makes use of the knowledge of the position of the satellite to introduce the proper delay.

# A PROGRESS REPORT ON SCINTILLATION OBSERVATIONS AT ANCÓN AND JICAMARCA OBSERVATORIES

## INTRODUCTION

The purpose of this report is to present a preliminary analysis of the data collected in connection with NASA contract work with ESSA (ESSA contract No. E22-9-70(N)). Under this contract a study of equatorial ionospheric irregularities using satellite transmissions is being performed.

To carry out this study, the telemetry system of the Ancón Satellite Tracking Station is being used to receive 136.4 MHz transmission from the geostationary satellite ATS-3 on two spaced antennas. Whenever it is possible observations with the Jicamarca radar are also conducted coincident with those at Ancón.

The primary objective of this study is to relate these measurements to space diversity systems that will permit one to reduce the degradation of satellite transmissions during the presence of ionospheric irregularities. The data collected will also be used to improve our understanding of the physical causes of these irregularities.

The first part of this report includes an analysis of propagation through a layer of irregularities. The purpose of this analysis is to relate the mentioned measurements with geostationary satellites with those effects that are found on lower satellite transmissions.

In the second part a review of space diversity techniques is made. Finally, the third part includes a description of the data collection work and data processing; also, use is made of derivations of part one to analyze the information obtained.

## PROPAGATION THROUGH A LAYER OF IONOSPHERIC IRREGULARITIES

In space diversity systems the separation between antennas is chosen to minimize the probability of simultaneous fading of the received signals. This is obtained when the separation exceeds the correlation distance of fading on the ground.

For fadings of satellite signals caused by ionospheric irregularities, the correlation distances projected on the ground depend on both the altitude of the satellite and of the irregularities.

Jicamarca observations show that ionospheric irregularities have a layered structure. Thus a treatment of propagation of radio waves through layers of irregularities is required to relate correlation distances observed with a geostationary satellite to those distances observed by lower satellites. Although it is not uncommon to find multiple layers of irregularities, for the purpose of this report only one layer is considered as a first approximation to the problem, and a monographic study of what is known on propagation through a region of irregularities is made. In a future work propagation through multiple layers will be studied.

The problem of propagation through a region containing refractive index irregularities has been treated by Chernov (1961), Tatarski (1961), Yeh (1962), Budden (1965) and others. They arrived at equivalent solutions following different approaches.

In this monograph the problem of propagation through a layer of irregularities will be considered as a single scattering problem. The received signals will be considered as the sum of the direct signal,  $E_d$ , plus the signal scattered by the irregularities,  $E_s$ . Multiple scattering is neglected. The geometry of the problem is illustrated in Figure 1. Spherical waves are emitted by a source at P and received at Q after travelling through a layer of irregularities. The thickness of the layer is W and is of infinite extent in the x and y directions.

The direct signal at the receiver is:

$$E_d = \frac{E_0}{R} e^{j[\omega t - k R]} \quad (1)$$

where

$$R = \overline{PQ}$$

and the scattered signal can be computed as follows: From Stratton (1941) the far-zone fields produced by an electron with acceleration  $\ddot{x}$  is given by

$$E_\theta = \left( \frac{\mu_0 e}{4 \pi} \right) \frac{\sin \theta}{r} \ddot{x} \quad (2)$$

where

- $\mu_0$  is permeability of free space
- $e$  is the charge of an electron
- $r$ ,  $\theta$  and  $\phi$  are defined in Figure 2.

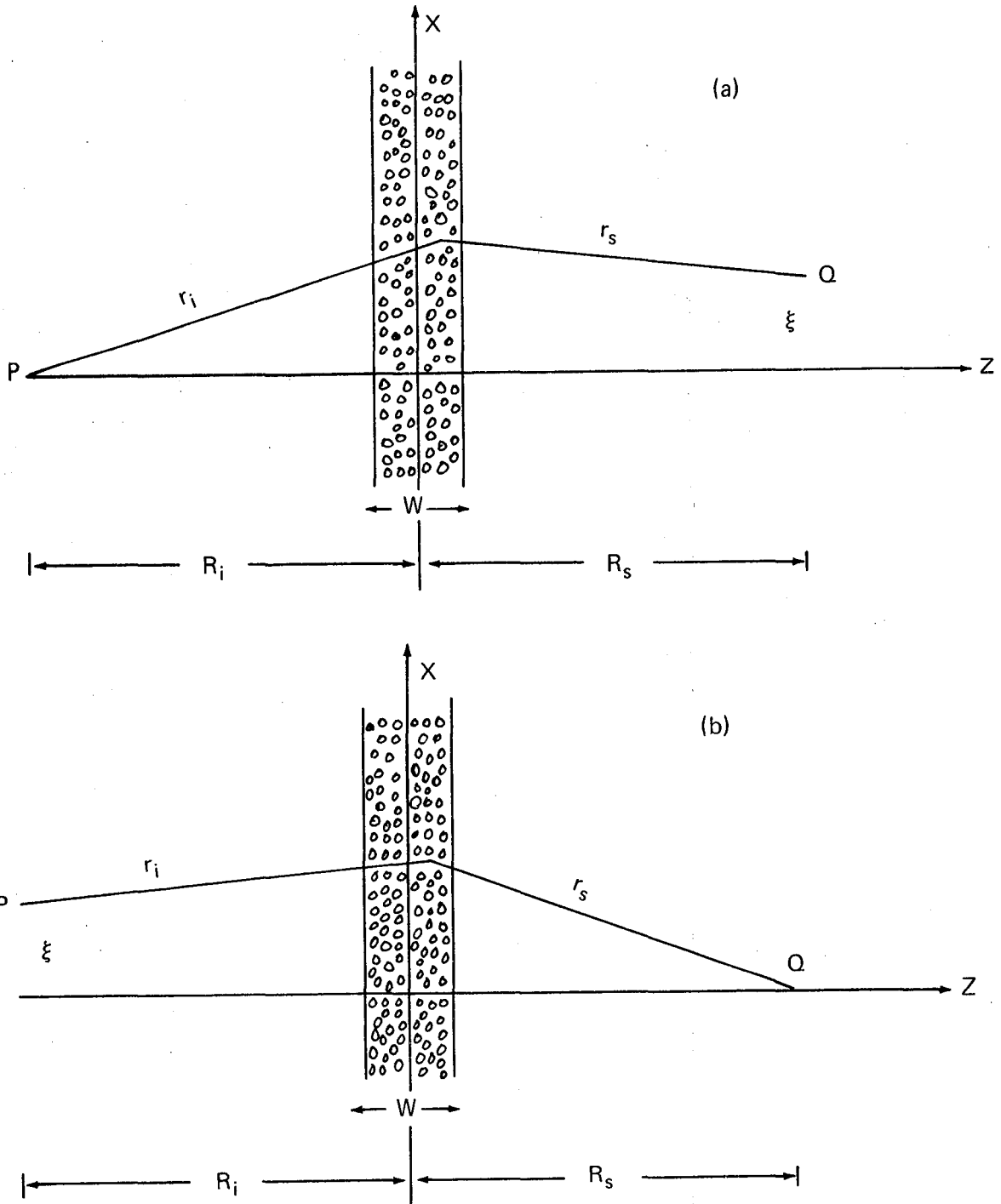


Figure 1. Geometry of scattering from a slab of ionospheric irregularities.  
 (a) Transmitter at  $\xi_m$  from Z axis. (b) Receiver at  $\xi_m$  from the Z axis.

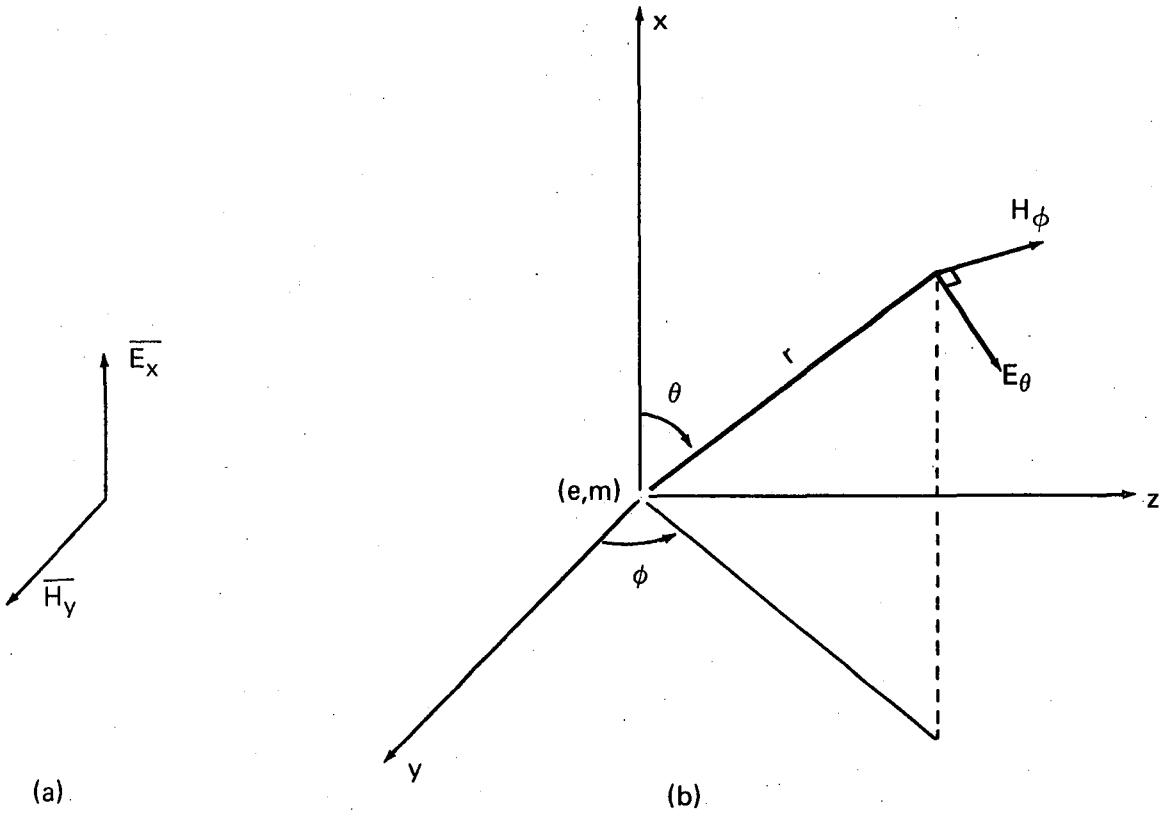


Figure 2. Geometrical parameters of scattering produced by nonrelativistic electron.

For non-relativistic velocities the acceleration of an electron due to an incident wave is mainly due to the electric field of the wave, that is

$$m \ddot{\mathbf{x}} = e \mathbf{E}_{\text{incident}} \quad (3)$$

Combining (2) and (3) we obtain for a single electron

$$\mathbf{E}_\theta = \frac{r_e}{r} \sin \theta \mathbf{E}_{\text{incident}} \quad (4)$$

where

$$r_e = \frac{\mu_0 e^2}{4\pi m}$$

Let the irregularities of the layer be characterized by a random variable  $\Delta N$  (x, y, z) electrons/ $m^3$  with average  $\overline{\Delta N} = 0$ . Then the field scattered by  $\overline{\Delta N}$  dv electrons is

$$d E_s (Q) = \frac{r_e}{r_s} \sin \theta E_{inc.} \Delta N d v \quad (5)$$

where

$r_s$  is defined in Figure 1.

and

$$E_{inc.} = \frac{E_0}{r_i} e^{j [\omega t - k r_i]} \quad (6)$$

If the typical scale size of the irregularities  $\ell \gg \lambda$ , then most of the field scattered will be confined to an angle  $\beta = \lambda/\ell$  measured from the direction of propagation. In the ionosphere  $\ell$  is in the order of 300 m and for a 136 MHz satellite signal,  $\lambda = 2.2$  m, then  $\beta$  will be of the order of  $0.4^\circ$ . Therefore, the angle  $\theta$  will be  $90^\circ + \beta \approx 90^\circ$  for most of the scattered field and

$$d E_s (Q) \approx \frac{r_e E_0}{r_s r_i} e^{j [\omega t - k (r_i + r_s)]} \Delta N d v \quad (7)$$

in integral form

$$E_s (Q) = r_e E_0 \int_{-W/2}^{W/2} \int_{-\infty}^{\infty} \int \frac{\Delta N}{r_i r_s} e^{j [\omega t - k (r_i + r_s)]} d x d y d z \quad (8)$$

Since the region of interest is confined to a small angle from the z axis in Figure 1, the usual approximation can be made. For the exponent part

$$r_i \approx (R_i + z) + \frac{x^2 + y^2}{2 (R_i + z)}$$

$$r_s \approx (R_s - z) + \frac{(x - \xi)^2 + y^2}{2 (R_i + z)}$$

where  $\xi$  is defined in Figure 1a, and for the denominator

$$r_i r_s \approx (R_i + z) (R_s - z)$$

then (8) becomes

$$E_s = r_e E_d \int \frac{\Delta N}{b} \exp \left\{ -j k \left[ \frac{y^2 + \left( x - \frac{\xi (R_i + z)}{R_i + R_s} \right)^2}{2 b} \right] \right\} d v \quad (9)$$

where

$$b = \frac{(R_i + z) (R_s - z)}{R_i + R_s}$$

$$d v = d x d y d z$$

Normalizing variables and lengths

$$x' = k x \quad y' = k y \quad z' = k z \quad b' = k b$$

$$w' = k w \quad R' = k R \quad R'_s = k R_s \quad \xi' = k \xi$$

gives

$$E = \frac{r_e E_d}{k^2} \iint \frac{\Delta N}{b'} \exp \left\{ -j \left[ \frac{y'^2 + \left( x' - \frac{\xi' (R'_i + z')}{R'_i + R'_s} \right)^2}{2 b'} \right] \right\} d v' \quad (10)$$

If the irregularities are assumed to be weak, then the scattered field is only a small fraction of the total field and the fluctuations are mainly due to the component of  $E_s$  in phase with  $E_d$ , Bowhill (1961). Let

$$A = \frac{R_e (E_s)}{E_d}$$

be the amplitude fluctuation coefficient, then

$$A(Q) \approx \frac{r_e}{k^2} \int \frac{\Delta N}{b'} \cos \left\{ \frac{y'^2 + \left[ x' - \frac{\xi' (R'_i + z')}{R'_i + R'_s} \right]^2}{2 b'} \right\} d v \quad (11)$$

This expression is similar to the one obtained by Yeh (1962), therefore, the results he obtained will be appropriated to obtain the mean signal value and correlation functions of the amplitude fluctuations. If the case of Figure 2b is considered it is found that

$$A(Q) \approx \frac{r_e}{k^2} \int \frac{\Delta N}{b'} \cos \left\{ \frac{y'^2 + \left[ x' - \frac{\xi' (R_s - z')}{R'_i + R'_s} \right]^2}{2 b'} \right\} d v \quad (12)$$

where if  $z$  is replaced by  $-z$  and  $y$  by  $-y$  it is found that the resulting expression is equal to the one that would be obtained if the source were placed at  $Q$  and the receiver at  $P$ . This could have been inferred from the reciprocity principle. To compute the mean square value of the amplitude fluctuations  $\xi$  can be taken equal zero to Figure 1a and

$$\overline{A^2} = \frac{r_e}{k^2} \overline{\Delta N^2} \iint \frac{\rho_{12}}{b'_1 b'_2} \cos \left( \frac{y_1'^2 + x_1'^2}{2 b'_1} \right) \cdot \cos \left( \frac{y_2'^2 + x_2'^2}{2 b'_2} \right) d v'_1 d v'_2 \quad (13)$$

where the bar indicates spatial average

$$\rho_{12} = \frac{\overline{\Delta N_1 \Delta N_2}}{\overline{\Delta N^2}}$$

In this expression spatial average have been taken as equivalent to ensemble average. Equation (13) can be transformed into

$$\overline{A^2} = 2 \left( \frac{r_e}{k^2} \right)^2 \overline{\Delta N^2} (I_1 + I_2) \quad (14)$$

where

$$I_1 = \iint \frac{\rho_{12}}{4 b'_1 b'_2} \cos \left( \frac{x_1'^2 + y_2'^2}{2 b'_1} - \frac{x_2'^2 + y_2'^2}{2 b'_2} \right) d v'_1 d v'_2$$

$$I_2 = \iint \frac{\rho_{12}}{4 b'_1 b'_2} \cos \left( \frac{x_1'^2 + y_1'^2}{2 b'_1} + \frac{x_2'^2 + y_2'^2}{2 b'_2} \right) d v'_1 d v'_2$$

assuming a Gaussian correlation function

$$\rho_{12} = \frac{\overline{\Delta N_1 \Delta N_2}}{\Delta N^2} = \exp - \left( \frac{x^2}{\ell_x^2} + \frac{y^2}{\ell_y^2} + \frac{z^2}{\ell_z^2} \right) \quad (15)$$

where  $\ell_x$ ,  $\ell_y$  and  $\ell_z$  are characteristic lengths, or correlation distances, in the x, y and z directions.

Using results obtained by Yeh (1962)

$$I_1 = W' \pi^{5/2} \ell_z \quad (16)$$

$$I_2 = - W' \pi \ell_z \int_{R'_i - W'/2}^{R'_i + W'_2} \sqrt{\frac{\pi^3 [(1 + D_x^2)^{1/2} (1 + D_y^2) + (1 - D_x D_y)]}{2 (1 + D_x^2) (1 + D_y^2)}} d \gamma' \quad (17)$$

where

$$\begin{aligned} \gamma' &= \frac{(R'_i + z'_1) + (R'_i + z'_2)}{2} \\ D_x &= \frac{4 \gamma' (R'_i + R'_s - \gamma')}{\ell_x'^2 (R'_i + R'_s)} \\ D_y &= \frac{4 \gamma'_i (R'_i + R'_s - \gamma')}{\ell_y'^2 (R'_i + R'_s)} \end{aligned}$$

The D's are equivalent to the wave parameter defined by Chernow (1961). If the layer is considered to be thin the D's will not change appreciable between the limits of integral (17) and mean values can be assumed and taken outside the integral. Let the mean values be

$$\bar{D}_x = \frac{4 R_i R_s}{k \ell_x^2 (R_i + R_s)}$$

$$\bar{D}_y = \frac{4 R_i R_s}{k \ell_y^2 (R_i + R_s)}$$

then (17) becomes

$$I_2 \approx -W' \pi^{5/2} \ell_z' \left[ \frac{\sqrt{(1 + \bar{D}_x^2) (1 + \alpha^2 \bar{D}_x^2)} + (1 - \alpha \bar{D}_x^2)}{2 (1 + \bar{D}_x^2) (1 + \alpha^2 \bar{D}_x^2)} \right]^{1/2} \quad (18)$$

where

$$\alpha = \frac{\bar{D}_y}{\bar{D}_x} = \left( \frac{\ell_x}{\ell_y} \right)^2$$

Finally using (16) and (18) in (13)

$$\overline{A^2} = 2 \left( \frac{r_e}{k^2} \right)^2 \overline{\Delta N^2} k^2 W \pi^{5/2} \ell_z' \left\{ 1 - \left[ \frac{\sqrt{(1 + \bar{D}_x^2) (1 + \alpha^2 \bar{D}_x^2)} + (1 - \alpha \bar{D}_x \bar{D}_y)}{2 (1 + \bar{D}_x^2) (1 + \alpha^2 \bar{D}_x^2)} \right] \right\} \quad (19)$$

Now, if two receiving antennas at  $Q_1 (\xi/2, 0, R_s)$  and  $Q_2 (-\xi/2, 0, R)$  are considered, the correlation function  $\overline{A(Q_1) A(Q_2)}$  can be obtained using (10)

$$\overline{A(Q_1) A(Q_2)} = \left( \frac{r_e}{k^2} \right)^2 \overline{\Delta N^2} \iint \frac{\rho_{12}}{b_1' b_2'} \cos(\Phi_1) \cdot \cos(\Phi_2) d v_1' d v_2' \quad (20)$$

where

$$\Phi_m = \cos \left\{ \frac{y_m'^2 + \left[ x_m' - \frac{\xi' (R_i' + Z_m')}{2 (R_i' + R_s')} \right]^2}{2 b_m'} \right\}$$

$$m = 1, 2$$

Let

$$\rho_A = \frac{\overline{A(Q_1) A(Q_2)}}{\overline{A(Q)^2}}$$

be the normalized transverse correlation function of A. The same procedure used to find  $\overline{A^2}$  can be used (Yeh, 1962) to find

$$\rho_A = \frac{I_3 + I_4}{I_1 + I_2} \quad (21)$$

where

$$I_3 = \int \int \frac{\rho_{12}}{4 b'_1 b'_2} \cos(\Phi_1 - \Phi_2) d v'_1 d v'_2$$

$$I_4 = \int \int \frac{\rho_{12}}{4 b'_1 b'_2} \cos(\Phi_1 + \Phi_2) d v'_1 d v'_2$$

The solutions of  $I_3$  and  $I_4$  are:

$$I_3 = \frac{\pi^3 \ell'_z}{2 \beta} \left\{ \operatorname{erf} \left[ \beta \left( R'_i + \frac{W'}{2} \right) \right] - \operatorname{erf} \left[ \beta \left( R'_i - \frac{W'}{2} \right) \right] \right\} \quad (22)$$

$$I_4 = -\frac{\pi^3 \ell'_z}{2 \beta} \operatorname{Im} \left\{ j (1 + j \alpha \bar{D}_x)^{-1/2} \left[ \operatorname{erf} \left( \frac{\beta \left( R'_i + \frac{W'}{2} \right)}{(1 + j \bar{D}_x)^{1/2}} \right) \right] - \operatorname{erf} \left[ \frac{\beta \left( R'_i - \frac{W'}{2} \right)}{(1 + j \bar{D}_x)^{1/2}} \right] \right\}$$

where

$$\beta = \frac{\xi'}{\ell'_x (R'_i + R'_s)}$$

Expressions (22) and (23) show that in general the correlation function,  $\rho_A$ , of the amplitude fluctuations do not have the same shape as the correlation function,  $\rho_{12}$ , of the ionospheric irregularities. Two asymptotic cases,  $\bar{D}_x \gg 1$  and  $\bar{D}_x \ll 1$ , can be used to illustrate this point. For  $\bar{D}_x \gg 1$  it is obtained

$$\overline{A^2} \approx 2 \left( \frac{r_e}{k^2} \right)^2 \overline{\Delta N^2} k^2 W \pi^{5/2} \ell_z \quad (24)$$

$$\rho_A \approx \exp \left[ - \frac{\xi^2}{(M \ell_x)^2} \right] \quad (25)$$

where

$$M = (R_i + R_s)/R_i$$

For  $\bar{D}_x \ll 1$

$$\overline{A^2} \approx \frac{3}{4} \left( \frac{r_e}{k^2} \right)^2 \overline{\Delta N^2} k^2 W \pi^{5/2} \ell_z \bar{D}_x^2 \quad (26)$$

$$\rho_A \approx \left[ 1 - 4 \left( \frac{\xi}{M \ell_x} \right)^2 + \frac{4}{3} \left( \frac{\xi}{M \ell_x} \right)^4 \right] \exp \left[ - \frac{\xi^2}{(M \ell_x)^2} \right] \quad (27)$$

Expressions (25) and (27) are approximately Gaussian and have characteristic lengths of the order of  $M \ell_x$ . Intermediate cases produce characteristic lengths which do not depart much from the two extreme cases (Bowhill, 1961). This permits us to use equations (25) and (27) as a first approximation to the problem of finding characteristic lengths of the ionospheric irregularities from satellite transmission, although  $\bar{D}_x$  do not depart much from unity.

At the magnetic equator ionospheric irregularities that cause amplitude scintillations of satellite signals are elongated along the earth's magnetic field lines with elongation ratios of 30 to 60. The small dimension of the diffraction pattern is of the order of 225 m and the irregularities appear at an altitude of the order of 300 km (Koster, 1967). If the longest direction is taken along the y axis of Figure 1 then an elongation ratio of 30 gives  $\alpha \approx 10^{-3}$ . For this value of  $\alpha$  equations (19) and (21) show that  $\overline{A^2}$  and  $\rho_A$  are approximately independent of  $\alpha$ . This means that scintillations at the equator are mainly due to the dimension of the irregularities perpendicular to the earth's magnetic field. This

causes the time variations of amplitude fluctuations due to a drifting layer of irregularities to be mainly due to the EW component of the drift.

Two cases will now be considered, the case of transmissions from a synchronous satellite and the case of transmissions from a lower satellite. The parameters listed in the first column of Table I will be used.

For a synchronous satellite the transmitted radio waves are practically plane when they are incident on the layer of irregularities. The projected correlation distances on the ground are approximately equal to those on the ionosphere. This is expressed by the fact that  $M \approx 1$ . Then in this case the value of  $\rho_x$  can be obtained from the correlation function  $\rho_A$ .

The fact that the ionospheric irregularities are drifting will permit one to measure  $\rho_A(\xi)$  from the time auto- and cross-correlation functions,  $\rho_A(\tau)$  and  $\rho_{A_1 A_2}(\tau)$ . This can be shown as follows: Assuming that the drifting irregularities do not change appreciable during a time  $\tau_0 = \ell_x / v_D$ , where  $v_D$  is the component of the drift velocity in the EW direction, then the field measured at the point  $Q_1(0, 0, R_s)$  at  $t = t_0$  will be the same as the field measured at  $Q_2(\xi, 0, R_s)$  at time  $t = t_0 + \xi / v_D$ . These arguments show that for the case of a synchronous satellite the time autocorrelation of the fluctuating signal is given by

$$\rho_A(\tau) \approx \exp \left[ - \frac{\tau^2}{\left( \frac{\ell_x}{v_D} \right)^2} \right] \quad (28)$$

Using the same arguments, the cross correlation of signals received at  $Q_1$  and  $Q_2$  will be given by

$$\rho_{A_1 A_2}(\tau) \approx \exp \left[ - \frac{(\tau - \tau_m)^2}{\left( \frac{\ell_x}{v_D} \right)^2} \right] \quad (29)$$

where

$$\tau_m = \frac{\xi}{v_D}$$

Then two antennas spaced  $\xi$  permit us to determine  $v_D$ , the EW component of the drift velocity, by measuring  $\tau_m$ . Knowing  $v_D$  it is then possible to determine  $\ell_x$  from the time correlation function.

Table 1  
Magnification Factors and Relative Power for  
Satellites at Different Heights

| $R_i + R_s$<br>Km | $\bar{D}_x$<br>Km | M<br>Km | $\bar{A}_{R_i + R_s}^2$<br>A |
|-------------------|-------------------|---------|------------------------------|
| 36,000            | 8                 | 1       | 0 db                         |
| 600               | 4                 | 2.2     | -0.8 db                      |
| 500               | 3.3               | 2.5     | -0.9 db                      |
| 400               | 2.1               | 4.0     | -2 db                        |
| 325               | 0.6               | 13      | -20 db                       |

Note: Quantities in Table I are for the following assumed parameters

$$\begin{aligned}
 R &= 300 \text{ km} \\
 \ell_x &= 225 \text{ km} \\
 W &= 50 \text{ km} \\
 f &= 136 \text{ MHz}
 \end{aligned}$$

The time  $\tau_0 = \ell_x / u_D$  determines the rate of fading of amplitude fluctuations.

For the case of a satellite at an altitude of the order of 600 km,  $D_x \approx 4$ . If a circular orbit is assumed, its velocity will be  $u_s \approx 7.8 \times 10^3$  m/sec. Since the drifting velocity of the ionosphere is in the order of  $10^2$  m/sec it can be assumed that during a time  $\tau$  of the order of  $(\ell_x / u_s)$  the ionosphere is static and the time variation of the signals are only due to the satellite movement. As it was pointed out this case can be studied by assuming that the transmitter is on the ground and that the receiver is at the satellite, then using equation (25)

$$\rho_A(\tau) \approx \exp \left[ - \frac{\tau^2}{\left( M' \frac{\ell_x^2}{v_s^2} \right)} \right] \quad (30)$$

where

$$M' = \frac{R_i + R_s}{R_s}$$

If equations (19), (25) and (27) are used for a different satellite altitudes Table I is obtained.

This table shows that as the satellite gets near to the layer of irregularities the fluctuations of amplitude decrease, but the spacecraft has to be very close to the layer for a substantial reduction.

## DIVERSITY COMBINING TECHNIQUES

Space diversity techniques can be used to improve the signal to noise ratio which suffers degradation by ionospheric irregularities. Diversity combining techniques can be studied in a general way to include polarization, frequency, space and other types of diversity systems. Here a brief review of this subject is made.

Diversity combining techniques has been studied for many years. Brennan (1959) made an analysis of three of the most used techniques: selection diversity, maximal ratio diversity and equal gain diversity.

In selection diversity the best of  $N$  noisy signals is chosen and used at a given instant of time.

In maximal ratio diversity the output is given by

$$f(t) = \sum_{i=1}^N a_i f_i(t)$$

where

$f_i$  is one of  $N$  noisy signals

$$a_i = \frac{\text{rms (signal)}}{\text{mean square (noise)}}$$

In equal gain diversity we have

$$f(t) = \sum_{i=1}^N f_i(t)$$

One conclusion from Brennan's study is that for  $N = 2$  all three types of diversity techniques give similar improvement.

In communication systems the reliability of a link is defined as the percentage of time a prescribed signal level is exceeded. Brennan defines diversity gain as the reduction in signal level obtained for a diversity system for a given reliability.

High reliability systems are designed for 99 to 99.9% reliability. If the power fluctuations are Rayleigh distributed then the diversity gains shown in Table II are obtained.

Table II  
Diversity Gain for 99% Reliability (Brennan, 1959)

| N | Selection | Equal Gain | Maximal Ratio |
|---|-----------|------------|---------------|
| 2 | 10        | 11         | 12            |
| 3 | 14        | 16         | 16.5          |
| 4 | 16        | 18.5       | 19.5          |

Table II shows that for  $N = 2$  satellite transmitter power reduction of 10 db can be obtained for a high reliability link. For lower reliability the diversity gain is reduced; at 50% reliability a reduction of power of the order of 3 db is possible.

Table II results were obtained under the assumption that the signals are uncorrelated and that there is no phase difference between the signals  $f_i$ .

Brennan found that cross correlations above 0.3 produce negligible results and that phase differences below  $37.5^\circ$  produce signal degradations effects. In the case under study the antennas should be separated so that the cross correlations of signals received simultaneously by the two antennas is smaller than 0.3. Then any of the combining techniques mentioned can be used to improve the signal to noise ratio.

For large separations of the antennas, the problem of phase difference between the signals exists. This difference depends on satellite position as shown in Figure 3 and is given  $d \sin \theta / \lambda_i$ , where  $\lambda_i$  is the minimum length of the information.  $\lambda_i$  is defined by the information bandwidth. For example, if the bandwidth is 300 kHz,  $d = 1$  km then  $\theta$  should be greater than  $45^\circ$  to keep the phase difference below  $37.5^\circ$ .

To record the signals from a satellite its angular position has to be determined either by manual or automatic track, therefore, the phase difference between the signals that arrive at separated antennas can always be approximated. Then, degradation caused by phase differences can be reduced to negligible values.

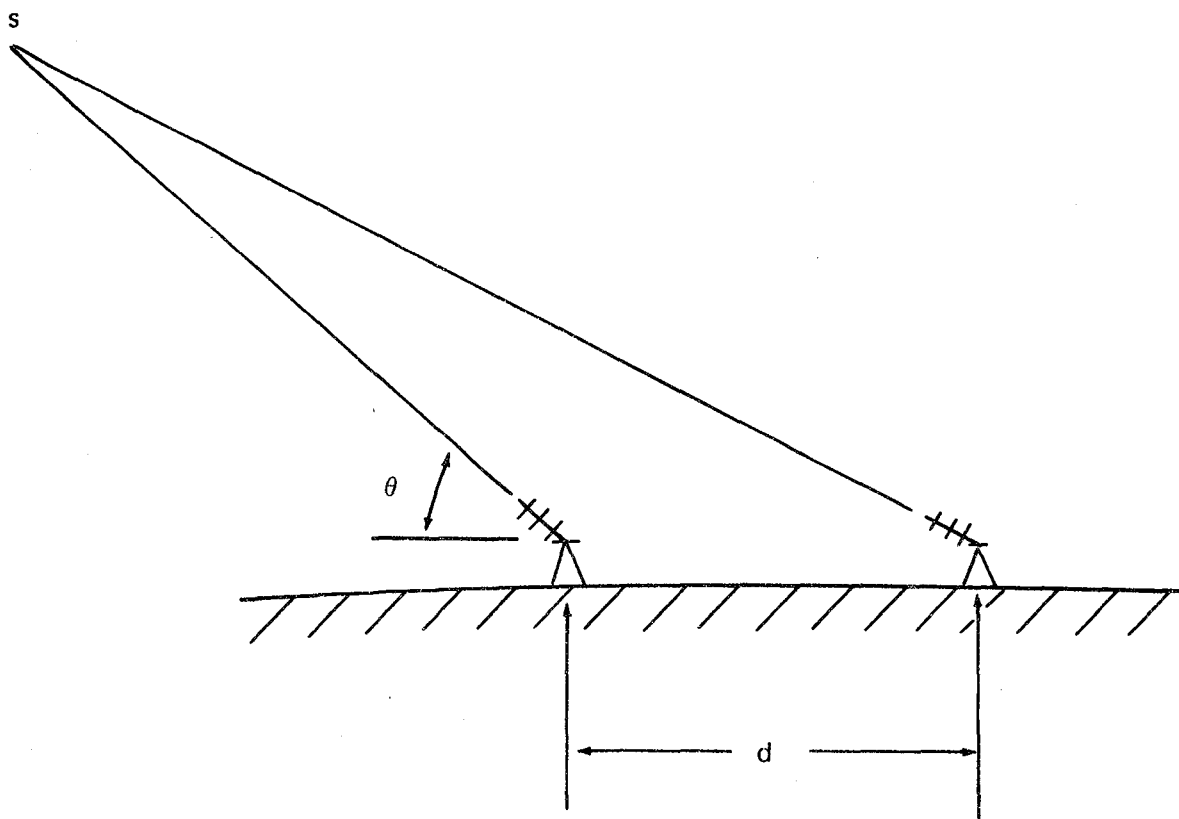


Figure 3. Signals from infinity received by two spaced antennas have a phase difference

$$\frac{d \sin \theta}{\lambda_i}$$

## ANALYSIS OF DATA

Scintillation data was recorded at Ancón from the beginning of 1970. The data was collected for two users, NASA and the Instituto Geofísico del Perú. To date there is a total of 45 recordings for the purpose of this experiment. Most of the data collected during the months of March and April correspond to one of the peaks of scintillation activity (Tisnado, et al, 1970).

Figure 4 shows a block diagram of the equipment used in this experiment. The antennas were oriented in an East-West direction and spaced 366 m. ATS-3 satellite transmissions distorted by the ionosphere were received and recorded in magnetic tape.

The magnetic tapes are then taken to Jicamarca Radar Observatory where the computing facilities are used. Figure 5 illustrates the processing system. The signals corresponding to the East and West antennas are played back in a FR-600

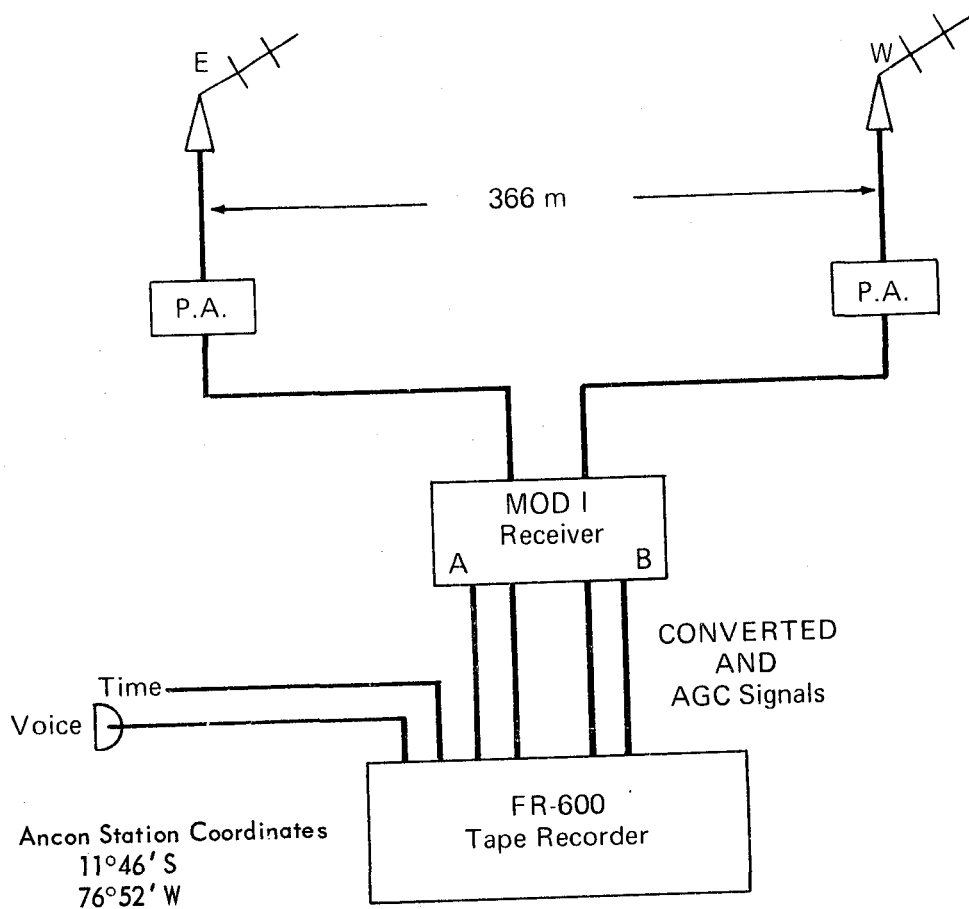


Figure 4. Block diagram of equipment used to gather scintillation data.

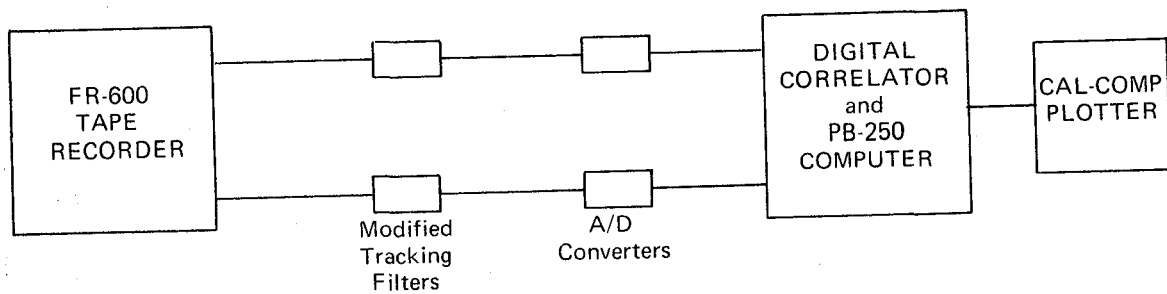


Figure 5. Block diagram of processing equipment for scintillation data.

tape recorder and fed to a pair of tracking filters where the signals are synchronous detected. This type of detection was chosen for its improved sensitivity and linear response which permits the observations of low amplitude fluctuations with sufficient resolution. The detected signals are then digitized and fed to the Jicamarca digital correlator which computes the autocorrelation function corresponding to each antenna and the cross correlation function between the antennas. The resulting information, after 3 minutes of integration time, is fed to the PB-250 for normalization and plotting. While the PB-250 is plotting, the computation of another set of functions is being done by the correlator, thus one set of functions can be plotted every 3 minutes.

The following standard expressions were used to compute the auto- and cross-correlation functions

$$\rho_A(\tau_i) = \frac{\sum_{i=1}^N (E_i - \bar{E})(E_{i+j} - \bar{E})}{\sqrt{\sum_{i=1}^N (E_i' - \bar{E})^2 \sum_{i=1}^N (E_i'' - \bar{E})^2}}$$

where

$E'$  and  $E''$  is the signal amplitude of an antenna

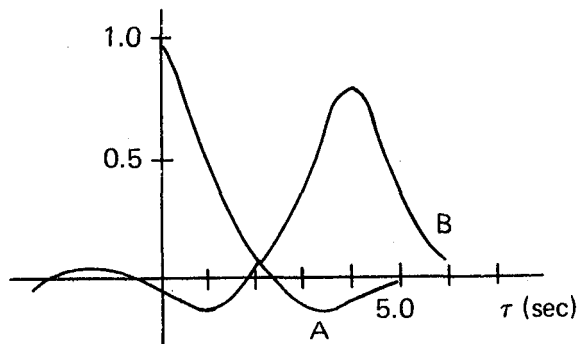
$\bar{E}$  is the average signal amplitude

$$\rho_{A'A''}(\tau_i) = \frac{\sum_{i=1}^N (E_i' - \bar{E}')(E_{i+j}'' - \bar{E}'')}{\sqrt{\sum_{i=1}^N (E_i' - \bar{E}')^2 \sum_{i=1}^N (E_i'' - \bar{E}'')^2}}$$

where  $E'$  and  $E''$  are signals corresponding to each of the antennas.

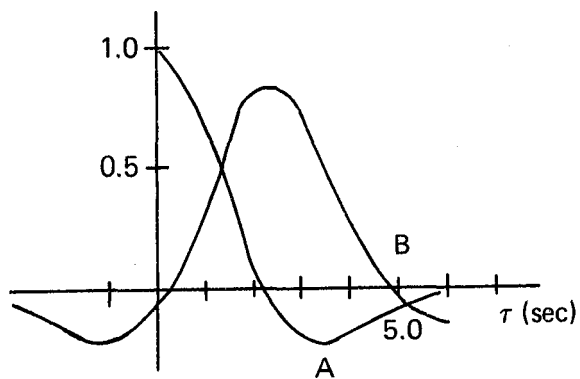
Figure 6 shows three typical correlation functions obtained. They are representative of what has been observed. The fact that the peak of the cross correlation functions is nearly unity, indicates that the ionospheric irregularities can be considered "frozen" as they pass over the antennas.

The width of the autocorrelation function,  $\tau_0$ , determines the fading rate and the scale sizes of the irregularities. The interval  $\tau_m$ , at which the maximum of the cross correlation occurs, determines the East-West component of the drift velocity of irregularities. To obtain this information, Gaussian functions were fitted to the auto- and cross-correlation functions, then equations (28) and (29)

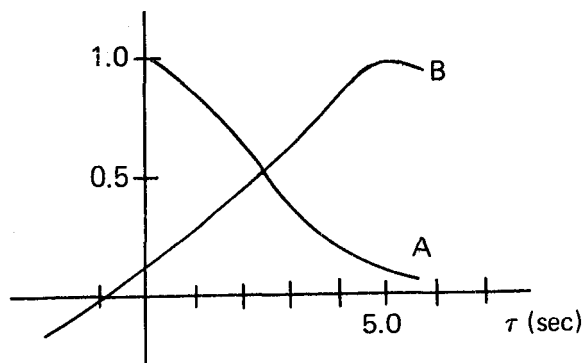


APRIL 4  
01.16.30 L.T.

A - Autocorrelation  
B - Crosscorrelation



AUGUST 29  
19.25.30 L.T.



MAY 30  
01.10.10 L.T.

Figure 6. Three typical auto and crosscorrelation signals.

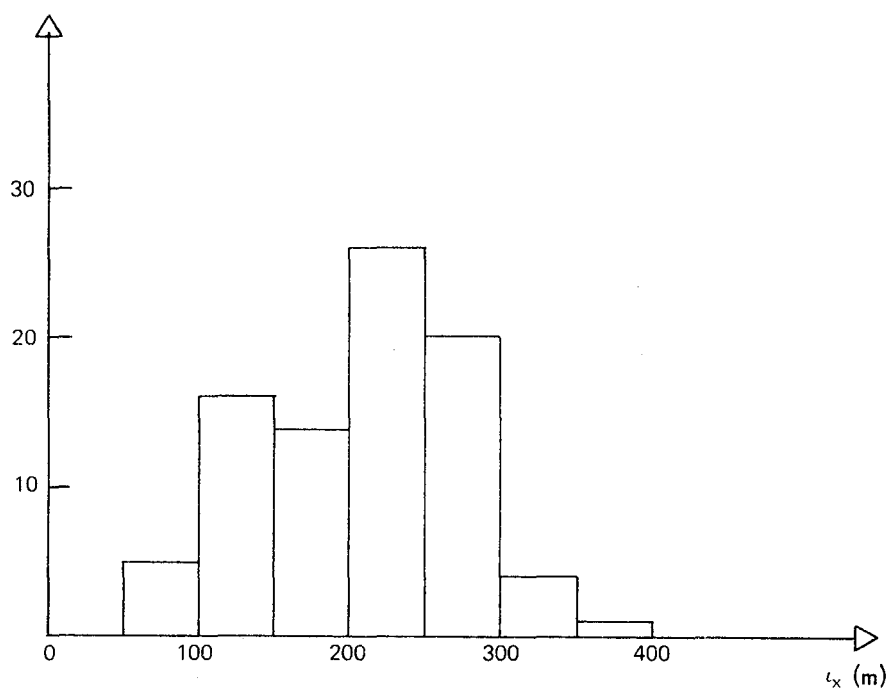


Figure 7. Distribution of scale sizes of irregularities.

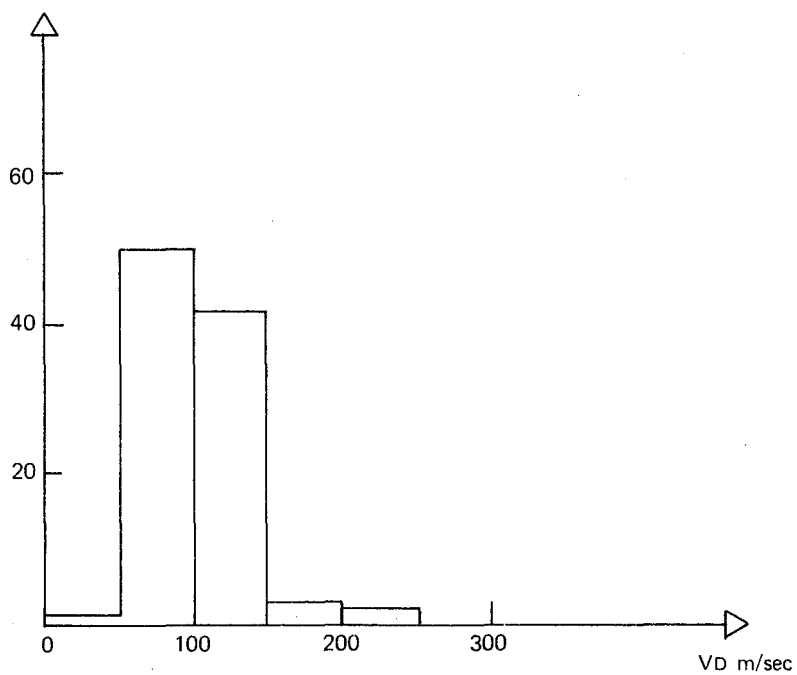


Figure 8. Distribution of W-E drift velocities.

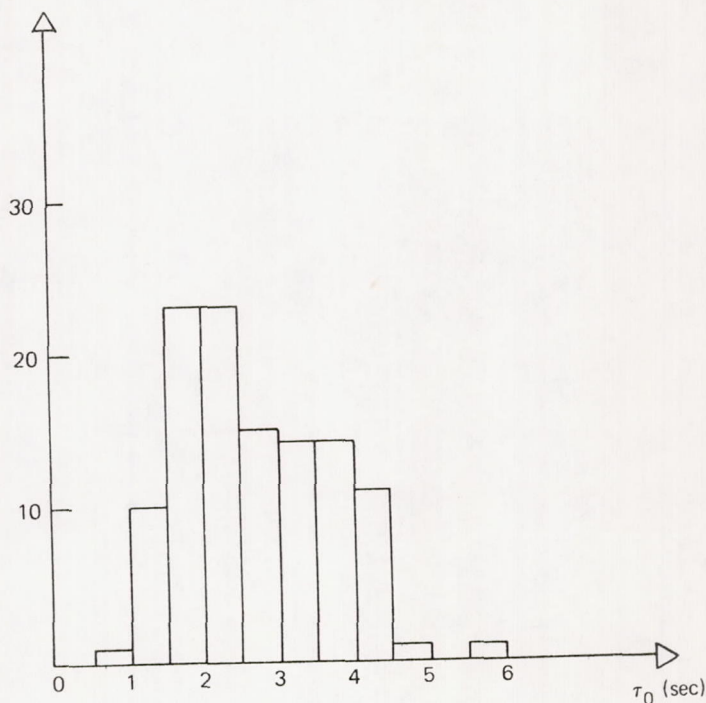


Figure 9. Distribution of correlation times.

were used. First,  $V_D$ , the East-West component of the drift velocity is computed from  $\tau_m$  taking  $V_D = 366 \text{ m}/\tau_m$ ; next the correlation length  $\ell_x$  is completed from  $\tau_0$  and  $V_D$  tracking  $\ell_x = V_D \cdot \tau_0$ .

The result of these computations are presented in Figures 7, 8, and 9 which show the distribution of correlation length, West to East drift velocity, and correlation width.

As it was mentioned earlier in this report the height of the irregularities is an important parameter in the design of space diversity systems, since the correlation distance on the ground will depend on it for low orbiting satellites. To obtain the height information of the irregularities observations are being conducted with the Jicamarca Radar. The layered structure of the irregularities is clearly established with these observations. Figures 10 and 11 show two typical film records obtained with the Jicamarca radar.

The case of multiple layers is not uncommon but at this time it has not been established whether or not all the layers are affecting satellite transmissions. In many cases Ancón has reported no scintillations while in Jicamarca's records, irregularities were clearly present.

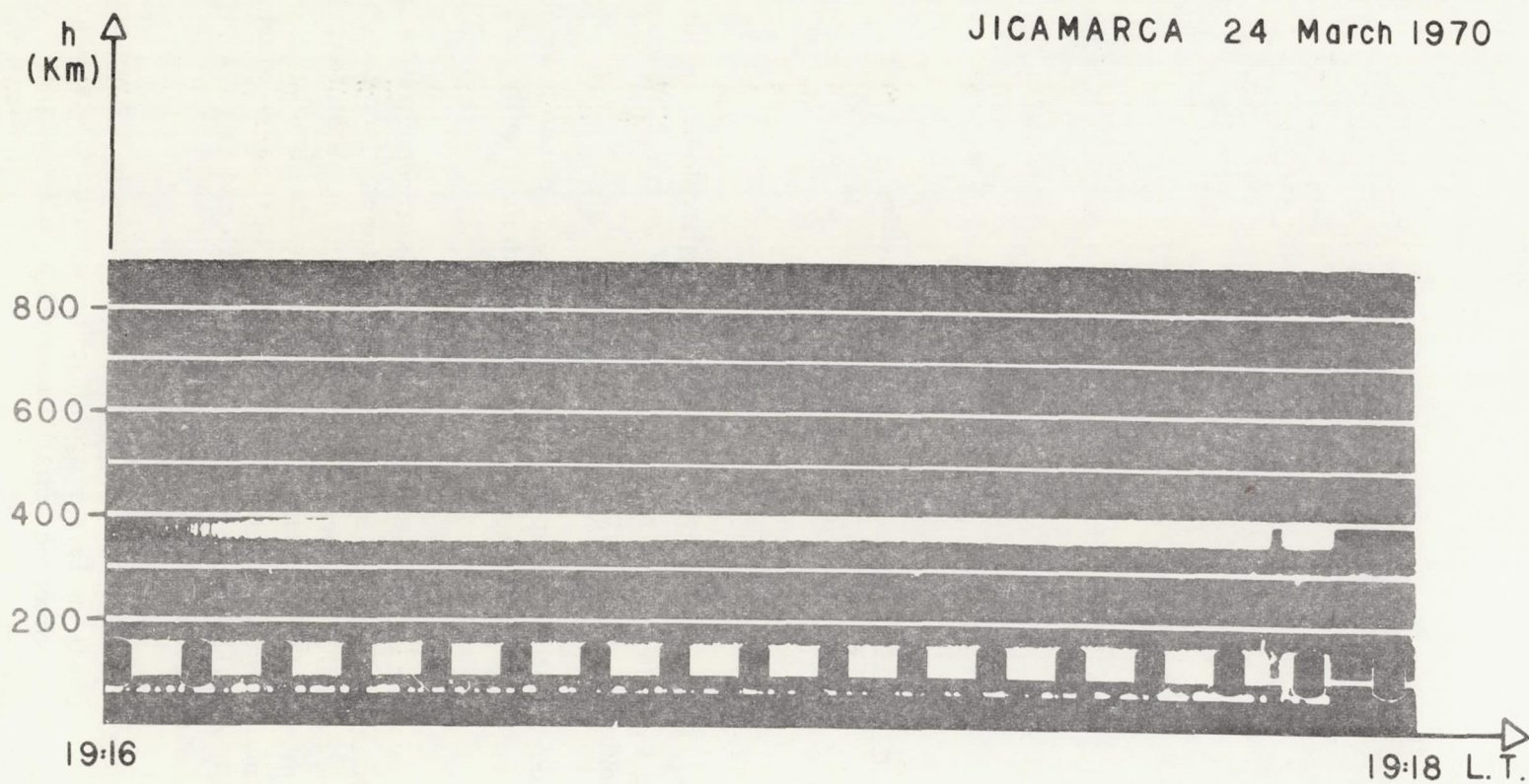


Figure 10. Typical radar observations of a layer of irregularities.

JICAMARCA 24 March 1970

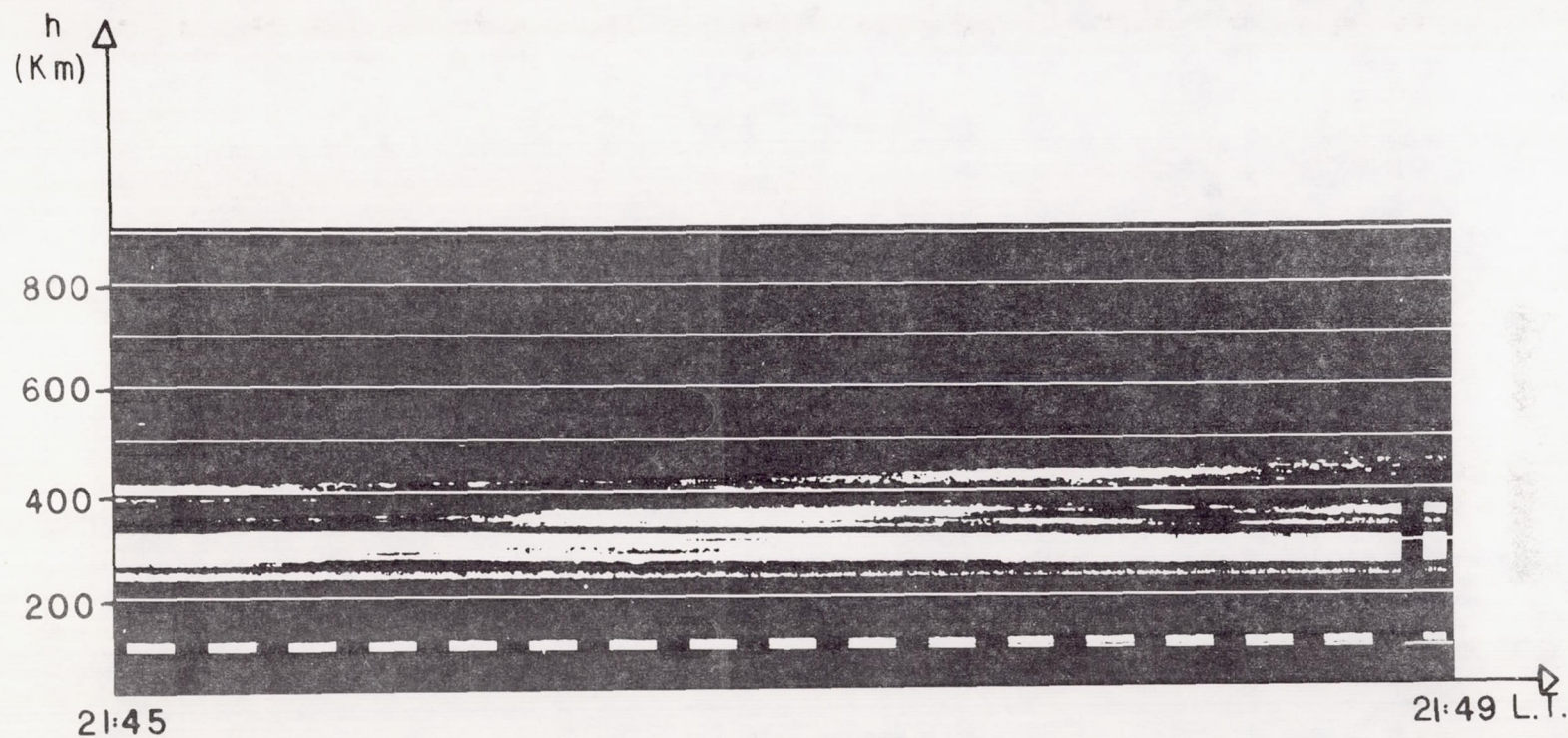


Figure 11. Typical radar observations of multiple layer of irregularities.

Figure 11.

At this time in Jicamarca a relative measurement of power reflected from the irregularities is being performed. It is hoped that this will permit a determination of the threshold at which satellite transmissions are affected.

There are two factors that have to be considered when comparing Jicamarca and Ancón measurements. First, both stations are not observing the same region of the ionosphere. Second, Jicamarca and Ancón are sensitive to different scale sizes of irregularities due to different operating frequencies.

## RECOMMENDATIONS FOR A SPACE DIVERSITY SYSTEM

Although it is still necessary to collect more data to improve the statistics of our results, some general recommendation can be given at this time about a space diversity system.

For synchronous satellites the spacing between antennas should be greater than 300 m to obtain low correlation. The low value of the cross correlation coefficient for  $t = 0$  in Figure 6 indicates that the separation of 366 m now in use at Ancón will be adequate for a diversity system.

For lower satellites the effect of magnification of the sizes determines that greater separation should be used. Since most of the satellites have altitudes above 500 km the estimated magnification factors are of the order of 3 as obtained from Table I. This gives separations of the order of 1 km which is not at all impractical. Except for practical limitations any reasonable distance above 1 km can be used for lower satellites. How far above one kilometer would depend on the percentage of reliability expected since there are times at which the irregularities exist at all heights in the range between 300 and 1000 km (Farley, et al, 1970).

Two practical problems associated with large separations are cable attenuation and phase differences between the signals. The problem of cable attenuation can be easily solved with the use of preamplifiers at both antennas to compensate for the losses. As was explained in this report phase differences due to ionospheric fading of satellite signals, in a space diversity system are a function of satellite time delay or position. The fact that this position is known permits one to compensate adequately for the phase differences with reasonable spacing.

It has been shown (Brennan, 1959) that the phase differences do not need to be compensated with high precision to permit us to solve this problem. As the satellite moves past the station the position information can be fed to a programmed device which will introduce in steps the appropriate phase shift or delay. Such a device has already been demonstrated by Goddard Space Flight Center.

## FUTURE WORK

The height of the irregularities that cause satellite scintillations is an important parameter since scale sizes on the ground depend on them. Simultaneous observations between Jicamarca and Ancón will be analyzed to obtain this information.

Lower satellites will be observed to measure the scale sizes and thus substantiate our estimations for the magnification parameter. These observations will be also used to estimate the height of the irregularities.

More tapes are being processed and more observations will be conducted during the September to December period of high scintillation activity. Time variation of drift velocity and scintillation index will be obtained. This will provide important information about the phenomenon.

Propagation through multiple layers will be studied and the distribution of amplitude fluctuations will be determined.

## REFERENCES

- Bowhill, S. A., Statistics of Radio Wave Diffracted by a Random Ionosphere, J. Res. Nat. Bur. Stand., D., Radio Propagation, 65D, 1961.
- Brennan, D. G., Linear Diversity Combining Techniques, Proc. IRE, 47, 1075-1102, 1959.
- Budden, K. G., The Amplitude of the Radio Wave Scattered from a Thick Ionospheric Layer with Weak Irregularities, J. Atmospheric Terrest. Phys., 27, 155-172, 1965.
- Farley, D. T., B. B. Balsley, R. F. Woodman, J. P. McClure, Equatorial Spread-F: Implications of VHF radar observations. Paper presented at USNC-URSI 1970 Spring Meeting, Washington, D. C. To be published.
- Chernov, L. A., Wave Propagation in a Random Medium, McGraw-Hill Book Co., New York, 1961.
- Coster, J. R., Studies of the Equatorial Ionosphere Using Transmissions from Active Satellites, Sci. Rept. AFCRL-68-0020, Sept. 1967.
- Tatarski, V. I., Wave Propagation in a Turbulent Medium, McGraw-Hill Book Co., New York, 1961.

Tisnado, G. R., R. Woodman and J. Pomalaza, Statistical Study of Equatorial Scintillations at Ancon, Peru. Instituto Geofisico del Peru, Internal Report, 1970.

Yeh, K. C., Propagation of Spherical Waves through an Ionosphere Containing Anisotropic Irregularities, J. Res. Nat. Bur. Stand., D., Radio Propagation, 66D, 621-636, 1962.